FT-IR Imaging of Polymer Dissolution by Solvent Mixtures. 3. Entangled Polymer Chains with Solvents

Beth A. Miller-Chou and Jack L. Koenig*

Department of Macromolecular Science, Case Western Reserve University, Cleveland, Ohio 44106

Received August 20, 2001

ABSTRACT: FT-IR imaging was used to study the dissolution of entangled poly(α-methylstyrene) (PAMS) in binary solvent mixtures of systematically varied amounts of methyl isobutyl ketone (MIBK) in deuterated cyclohexane (C_6D_{12}). FT-IR images and concentration profiles were obtained, and the results were compared and contrasted with the results of the previously reported unentangled system. It was found that, in many of the solvent systems, the solvent did not dissolve the polymer uniformly at the polymer−solvent interface, causing cracking and roughening of the polymer edge, which can be directly seen in the images. In addition, there was evidence of solvent segregation, which was not seen in the unentangled PAMS.

Introduction

The dissolution of glassy polymers has been the subject of many studies for some time and for good reason.[1−13] For example, polymer dissolution is of great interest in microlithography and the manufacturing of microchips and integrated circuits. The resist coatings can be subjected to varying degrees of radiation by placing a mask with the circuit pattern over a thin polymer film. Either a positive or a negative image of the original mask is formed, depending on the chemical nature of the photoresist. Negative resists will undergo cross-linking upon irradiation, and the areas with higher cross-link densities will have lower solubilities than those with lower cross-link densities. On the other hand positive resists undergo molecular changes that enhance their solubility in the solvent so that exposed regions are preferentially removed.[1] Therefore, different patterns can be generated on a substrate, and desired electrical characteristics of a circuit are achieved by selectively doping, metalizing, or insulating regions of the substrate.

Polymer dissolution with pure solvent systems has been extensively studied.[2−6] However, in many cases a mixture of solvents may be preferred, and there are several advantages of using a multisolvent mixture. For example, a less expensive solvent may be added to a more expensive solvent to cut down on the cost of overall solvent mixture. Also, binary solvent systems are used to achieve a high dissolution rate with minimal unwanted swelling or cracking, which can cause distortion of the desired resist patterns.

Several techniques have been used to study solvent ingress and dissolution of polymers. Krasicky et al. utilized laser interferometry to determine dissolution rates and monitor the transition layer during polymer dissolution.[7,8] Webb and Hall found that ingress rates of a binary solvent mixture were identical and intermediate between the two pure component rates via magnetic resonance imaging (MRI).[9] In addition, optical microscopy has been used successfully to study the swelling and dissolution behavior since it allows measurement of the rate of dissolution and observation of the concentration profile in the dissolving surface layer.[10,11] Rutherford backscattering spectroscopy has proven useful to study swelling as well.[12] Another technique, FT-IR imaging has also proven successful, as will be discussed later.[13] It is difficult to directly compare the results of these various techniques since different factors representing the same properties are produced, and there are different sources of error that can occur from technique to technique.

It is of particular interest to study polymer dissolution in situ. Ouano and Carothers studied PAMS and other polymers' dissolution dynamics in situ using a critical angle illumination technique.[10] They found that PAMS exhibited both a small amount of cracking and swelling. It was concluded that the dissolution dynamics of polymers depend on factors such as polymer tacticity, glass transition temperature, mechanical and thermal history, and solvent swelling power. Polymer dissolution in solvent mixtures of MIBK and cyclohexane-*d* was also monitored in situ with FT-IR imaging.[13] The PAMS was below the entanglement molecular weight, in contrast to our system where the polymer was above its entanglement molecular weight. The polymer dissolution rates of the unentangled PAMS were found to be approximately linear with time and concentration of MIBK in the solvent mixture, and the solvent diffusion was characterized as case II type diffusion. There was no evidence of solvent segregation and both solvents appeared to diffuse into the polymer at the same rate.

It is the goal of this study to determine and characterize the role of entanglement effects on the dissolution process, diffusion rates, and segregation of components using the same methods that were used to study the unentangled system. Therefore, direct comparisons and contrasts can be efficiently made. It was expected that swelling would occur and overall dissolution rates would decrease for the entangled PAMS.

Experimental Section

PAMS (M_n = 28 200; M_w = 31 400; T_g ~169 °C) was purchased from Scientific Polymer Products[14] and used as received. Solvents (cyclohexane-*d* (99.6% deuterated) and MIBK) were purchased from Aldrich Chemical Co.[15] and used as received in various weight ratios. FT-IR imaging experiments were conducted using the contact method which has been described elsewhere.[16] To prepare a thin layer of polymer sandwiched between two salt plates, a small amount of solid

10.1021/ma0115038 CCC: $22.00
Published on Web 12/12/2001

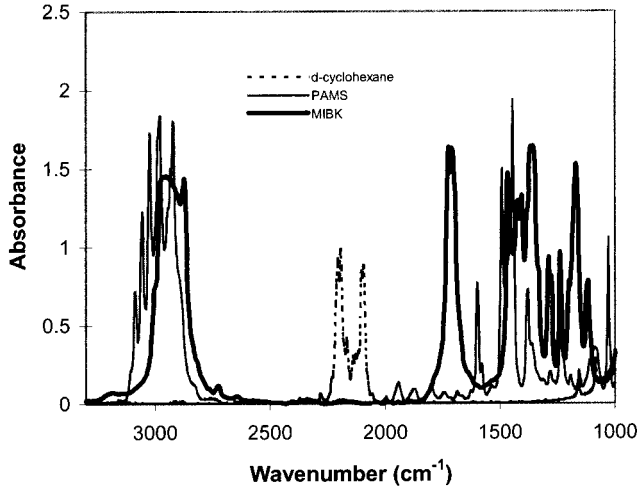

Figure 1. Spectra and peaks used to monitor each component in the system.

polymer was placed on a 2 mm thick CaF_2 substrate and was heated in an oven to 210 °C. Another substrate was then placed on top of the polymer, and a weight was applied on top of the substrate sandwich. The sample was kept in the oven overnight, after which it was allowed to cool in ambient air to room temperature. Solvent was introduced from the empty end after the sampled interface was positioned in the spectrometer. The solvent entered the space between the substrates due to capillary action and came into contact with the polymer. Images were sequentially acquired over a period of time as high as 106 min. Solvent solution was added as necessary.

Infrared images were acquired using the Bio-Rad Stingray[17] imaging spectrometer. The Stingray is comprised of an FTS 6000 step-scan interferometer bench coupled to a UMA-500 microscope accessory. The imaging detector is a Santa Barbara focal plane array of 64 × 64 mercury cadmium telluride (MCT) elements imaging an average spatial area of 400 μm × 400 μm in a single experiment. A long pass filter to eliminate unwanted wavelengths and prevent Fourier folding over perturbations was inserted into the beam path. An 8 cm^{-1} nominal spectral resolution and an undersampling ratio (UDR) of 4 were used for the study. A mirror stepping rate of 5 Hz was used to give a total scanning time of about 210 s. The number of camera frames (frame rate = 316 Hz; integration time = 0.0938 ms) averaged during each spectrometer step was 20. Image processing and data extraction were carried out using the hyperspectral imaging software package Environment for Visualizing Images (ENVI).[18] Reduced noise absorbance profiles were extracted from each image by averaging the spectral data from a 50 μm wide cross section of the image.

Each component of the system was monitored by a characteristic IR absorbance peak. Absorbance spectra for the neat solvent mixture components and polymer can be seen in Figure 1. The peak at 1600 cm^{-1}, representing the ring quadrant stretching mode, was used to characterize the polymer, and the peak at 1720 cm^{-1} (C=O stretching vibration) was used for MIBK. A peak edge of 2148 cm^{-1} (CD stretching) was used to monitor cyclohexane-*d*. The peak at 2100 cm^{-1}, which was used when studying the unentangled system, could not be used for this study because of overabsorbance that caused problems with quantitative data analysis and calculations. For an experiment where no overabsorbance occurred at 2100 cm^{-1}, results using 2148 and 2100 cm^{-1} for cyclohexane-*d* were compared, and they were found to produce the same qualitative and quantitative information. Therefore it was concluded that 2148 cm^{-1} could successfully be used to monitor the cyclohexane-*d*. Experiments were run using solvent mixtures with the following weight ratios of cyclohexane-*d* to MIBK: 100:0, 95:5, 90:10, 85:15, 80:20, and 0:100.

Results and Discussion

The dissolution of the entangled PAMS proved to be very different from the unentangled system. First, a very interesting phenomenon occurred when PAMS was

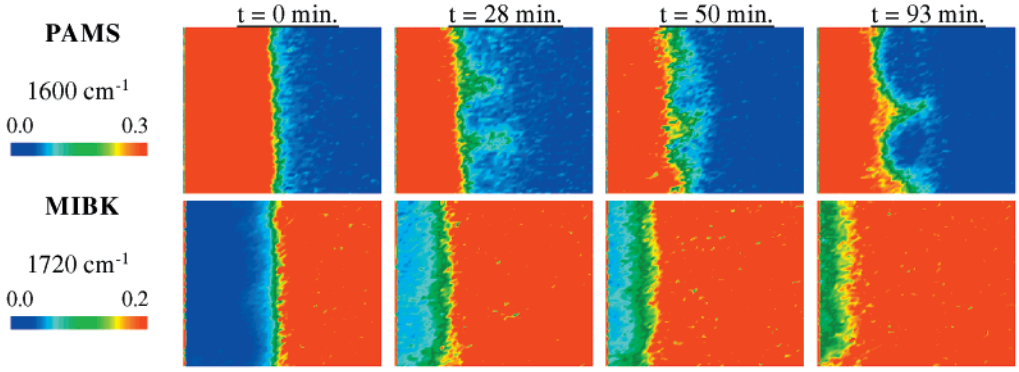

Figure 2. Spectral images showing the concentration of PAMS and MIBK during dissolution of PAMS.

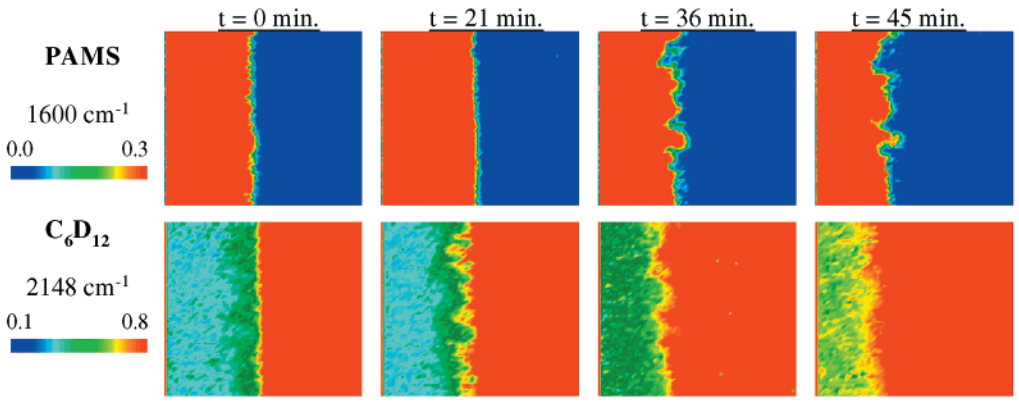

Figure 3. Spectral images showing the concentration of PAMS and cyclohexane-*d* during dissolution of PAMS.

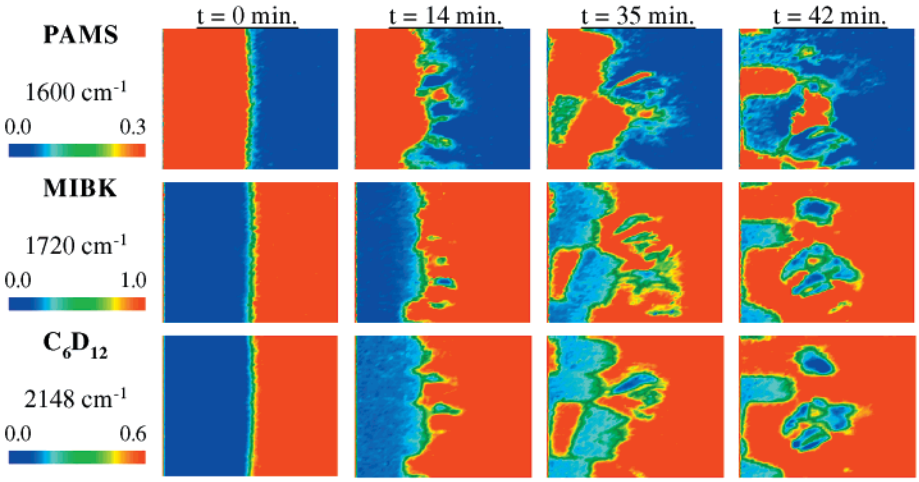

Figure 4. Spectral images showing the concentration of PAMS, MIBK, and cyclohexane-*d* during dissolution of PAMS in an 85:15 cyclohexane-*d*:MIBK solvent solution.

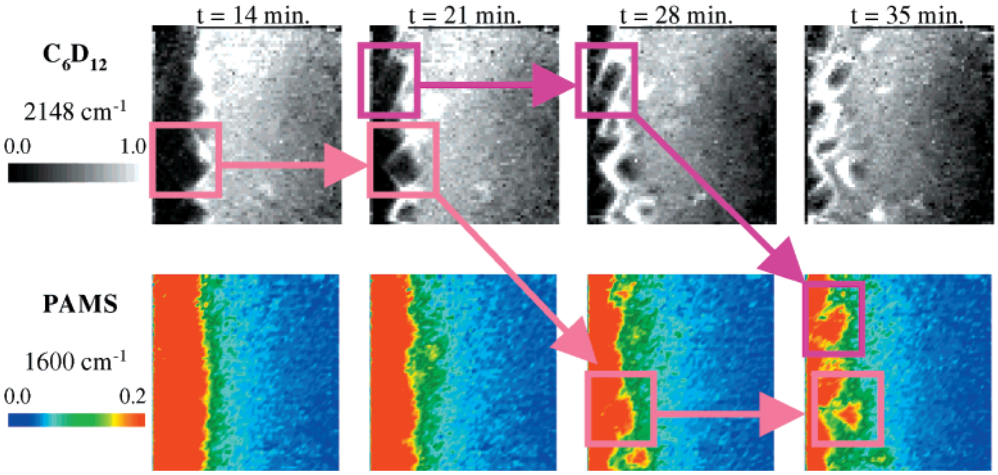

Figure 5. Spectral images showing the concentration of PAMS with corresponding black and white images of C_6D_{12} at the same time. When cracks meet, a polymer chunk breaks away from the bulk polymer.

dissolved with pure MIBK. Images obtained by plotting the characteristic absorbance frequency for each component are shown in Figure 2. Dissolution did not occur uniformly over the polymer−solvent interface, creating physical peaks and crevices. Small portions of polymer peeled away from the bulk polymer at different times. When the PAMS was tested with pure cyclohexane-*d*, a similar interface-roughening was observed, as shown in Figure 3.

With FT-IR imaging, concentration profiles can be used to calculate the polymer dissolution rate. The rate can be determined by monitoring the position of the polymer−solvent interface as a function of time. The velocity of the interface can be multiplied by the perpendicular area exposed to the solvent to obtain the dissolution rate.[13] However, since the polymer was not dissolving uniformly and produced a rough interface, the velocity of the interface could not accurately be calculated as it was for the unentangled system. The velocity calculated over one cross-section of the entangled polymer sample varied greatly in comparison to that of one calculated from another cross-section of the same sample. This also proved to be the case with the binary solvent mixtures.

An example of a mixed solvent experiment can be seen in Figure 4. It is very clear from these images that the polymer did not dissolve uniformly and blocks of polymer erupted from the bulk polymer interface. However, upon repeating the experiment, the polymer appeared to dissolve uniformly with only a slight roughening of the polymer−solvent interface. This was predominantly the case with the solvent mixtures: sometimes polymer pieces of various sizes would break away from the bulk, and at other times "normal" dissolution would occur. When one views the unbaselined black and white images of the experiments, it appeared that sharp cracks were forming at the polymer−solvent interface. When the cracks would meet, a piece of polymer would be late being released from the bulk polymer (Figure 5).

The cracks explain the randomness of pieces erupting from the bulk polymer. The eruption process depends on if and how the polymer cracks meet. If the cracks meet, then a block of polymer will break away from the bulk polymer. There was no evidence of this cracking phenomenon reported for the unentangled system. Ouano and Carothers also observed PAMS cracking during dissolution with a similar solvent, methylethyl ketone (MEK).[11] By comparing dissolution results of different polymers, they concluded that a polymer dissolves either by exhibiting a thick swollen layer or by undergoing extensive cracking, depending on how fast the osmotic pressure stress built up in the polymer matrix is relieved. Ueberreiter also reported a cracking

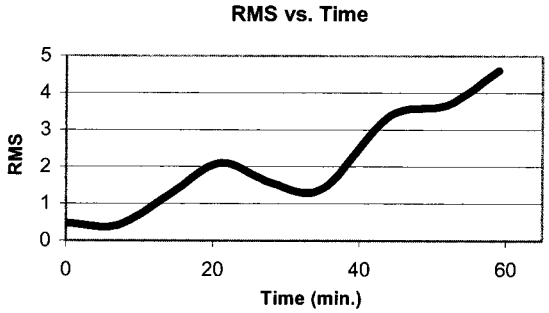

Figure 6. Typical plot of rms vs time for the dissolution of PAMS by a cyclohexane-*d*:MIBK solvent solution.

effect for poly(methyl methacrylate−dimethylphthalate).[10] He found that if the logarithm of the velocity of penetration was plotted vs the reciprocal of temperature, two breaks in the curve could be observed. The first break occurred at the glass transition temperature, and the second, more significant break occurred at the temperature at which a gel layer ceased to appear, termed the gel temperature. Cracks were observing running into the polymer matrix, and they combined and caused small blocks of the polymer to leave the surface in a kind of eruption process. This is the exact same effect we observed with our system. Ueberreiter and co-workers believed the reason for this process was the freezing-in of large amounts of stress energy in the polymer in the glass transition interval, and these stresses are probably mainly concentrated along the wider channels and hole systems which are created by the volume contraction due to the glass transformation process. The penetrating front of the solvent fills the largest holes and channels, thus attacking points of weakest cohesion. The theories of Ouano and Carothers and of Ueberreiter and co-workers can help to explain the phenomenon observed in our system. As the solvents ingress into the polymer, pressure builds up because of the limited segmental mobility of the entangled chains. Eventually, the pressure gets high enough that fracture occurs and relieves the stress. Most likely, cracks could not be seen in the unentangled system because (1) the pressure could be easily relieved since the unentangled chains are more mobile, and segmental mobility is high since the system was tested above the gel temperature, or (2) the cracks formed and propagated so fast that the polymer appeared, in the imaging time frame, to dissolve "normally".

The cracking process also explains the roughening of the polymer−solvent interface. When a crack forms, solvent can flow into the crack and dissolve polymer deeper within the bulk leaving behind an uneven surface. Müller-Buschbaum et al. used specular and off-specular X-ray scattering to study surface morphology and roughness of polystyrene films.[19] They found that the roughness and morphologies were determined by the vapor pressure of the solvents used to prepare the films. With increasing vapor pressure, the surface roughness increased. Cyclohexane-*d* and MIBK have vapor pressures of 95[20] and 16 mmHg,[21] respectively, at 20 °C. Therefore, there may be additional stress added to the system by the high vapor pressure of cyclohexane-*d*, which furthers the explanation of crack formation.

Since a roughening of the polymer surface was apparent, the root-mean-square roughness (rms) was calculated and plotted with time for each experiment. The equation for rms is

$$\mathrm{rms} = [\sum (Z_i - Z_{\mathrm{ave}})^2/N]^{1/2}$$

Z_i = height on the Z axis of a particular feature in topology

Z_{ave} = average height

N = number of pixels in the image

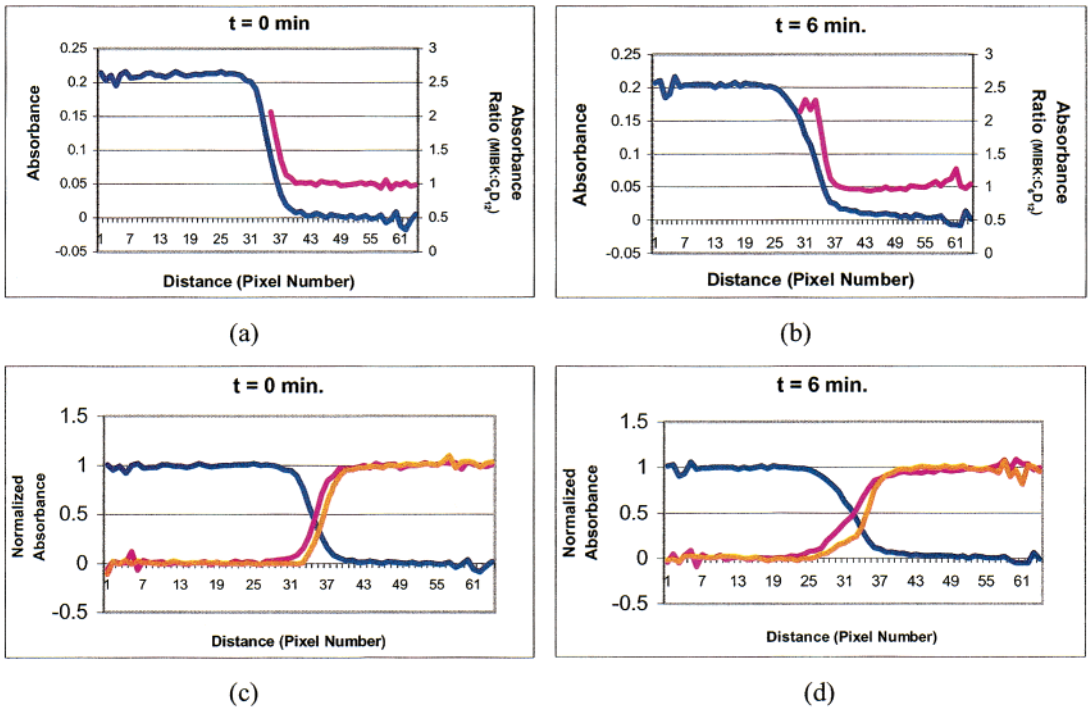

Figure 7. (a) Absorbance profile for the polymer and a profile of the ratio of the solvent mixture components' absorbance for a 95:5 cyclohexane-*d*:MIBK at the start of an experiment and (b) a similar plot for a time corresponding to 6 min of dissolution. (c) Normalized absorbance profiles at the same time as part a. (d) Normalized absorbance profiles at the same time as part b.

with the Z axis located horizontally within the image. For our setup, Z_i was the number of pixels in each row indicating bulk polymer and N was 64, the number of rows of pixels in an image. Figure 6 is a typical rms vs time graph for the dissolution images. An increase and decrease of rms occurred somewhere within the first 30 min of the experiment. This is most likely due to the random crack formation. When the cracks first propagate, the roughness increases, but as time proceeds, the sharp edges are smoothed out by the solvent, thus decreasing the rms from the rms value at the time when cracks first propagated.

Both solvents diffused into the unentangled PAMS at the same rate and the solution composition remained constant throughout the solvent solution. However, solvent segregation was observed for the dissolution of the entangled PAMS. Parts a and b of Figure 7 plot the values of the ratio of the absorbance of the two solvent peaks and the corresponding PAMS concentration profiles. The absorbance ratio (MIBK:cyclohexane-*d*) reflects the composition of the solvent solution. There is an increase in this profile at the polymer−solvent interface indicating that MIBK is diffusing into the polymer before the cyclohexane-*d*. Parts c and d of Figure 7 plot the normalized absorbance profiles for each component at the same time and for the same mixture in Figure 7, parts a and b. Clearly the MIBK diffuses into the PAMS first. This effect is most distinguishable with the 5% MIBK solvent mixture at early times in the experiment.

The idea of MIBK diffusing in first is not unexpected since its solubility parameter is closer to that of PAMS, and the sizes of the two solvents are similar. The solubility parameters of the system's components are 19.3, 16.8, and 17.2 $MPa^{1/2}$ for PAMS, cyclohexane-*d*, and MIBK, respectively.[22] Ribar et al. found that for the 5% MIBK solution, in particular, there was a large difference between the observed and predicted diffusion rates, and they theorized that the reason for this phenomenon was solvent segregation.[13] It is clear from our experiments that solvent segregation does indeed occur for this particular solvent mixture.

Conclusions

The dissolution of entangled PAMS is very different from unentangled PAMS. The polymer did not dissolve uniformly at the polymer−solvent interface. It appears that as the solvents ingress into the polymer, pressure builds up because of limited segmental mobility of the entangled chains and high vapor pressure of cyclohexane-*d*. Large amounts of stress energy are frozen into the polymer in the glass transition. This stress is relieved by cracking, and when the cracks combine, they cause small blocks of the polymer to break away from the bulk polymer. This was not seen in the unentangled system, most likely, because the T_g was much lower, and thus segmental mobility was much higher, such that stress can easily be relieved. This cracking caused a roughening of the polymer surface and the rms was calculated and plotted with time. The rms gave a numerical term to characterize the roughening caused by the cracks with time, and a trend could be seen. Last, solvent segregation was clearly seen in the 5% MIBK solvent mixture. The MIBK, which has a solubility parameter that is very close to that of PAMS, was present at higher concentrations at the polymer−solvent interface in the early stages of dissolution.

Acknowledgment. The authors would like to thank the Ohio Board of Regents and the National Science Foundation Center for Advanced Liquid Crystalline Optical Materials (ALCOM) for financial support, and Travis Ribar and Rohit Bhargava for their helpful discussions.

References and Notes

(1) Narasimhan, B.; Peppas, N. A. *Adv. Polym. Sci.* **1997**, *128*, 158−207.
(2) Thomas, N. L.; Windle, A. H. *Polymer* **1982**, *23*, 529−542.
(3) Mills, P. J.; Palmstrom, C. J.; Kramer, E. J. *J. Mater. Sci.* **1986**, *21*, 1479−1486.
(4) Weisenberger, L. A.; Koenig, J. L. *Macromolecules* **1990**, *23*, 2445−2453.
(5) Hyde, T. M.; Gladden, L. F.; Mackley, M. R.; Gao, P. *J. Polym. Sci., A, Polym. Chem.* **1995**, *33*, 1795−1806.
(6) Hassan, M. M.; Durning, C. J. *J. Polym. Sci., B, Polym. Phys.* **1999**, *37*, 3159−3171.
(7) Krasicky, P. D.; Groele, R. J.; Rodriguez, F. *J. Appl. Polym. Sci.* **1988**, *35*, 641−651.
(8) Krasicky, P. D.; Groele, R. J.; Jubinsky, J. A.; Rogdriguez, F. *Polym. Eng. Sci.* **1987**, *27*, 282−285.
(9) Webb, A. G.; Hall, L. D. *Polymer* **1991**, *32*, 2926−2938.
(10) Ueberreiter, K. In *Diffusion in Polymers*; Crank, J., Park, G. S., Eds.; Academic Press: New York, 1968.
(11) Ouano, A. C.; Carothers, J. A. *Polym. Eng. Sci.* **1980**, *20*, 160−166.
(12) Lasky, R. C. Ph.D. Thesis, Cornell University, 1986.
(13) Ribar, T. B.; Bhargava, R.; Koenig, J. L. *Macromolecules* **2000**, *33*, 8842−8849.
(14) Scientific Polymer Products, Inc., Ontario, NY.
(15) Aldrich Chemical Co., Milwaukee, WI.
(16) Challa, S. R.; Wang, S.-Q.; Koenig, J. L. *Appl. Spectrosc.* **1996**, *50*, 1339−1344.
(17) Bio-Rad, Digilab Laboratories, Cambridge, MA.
(18) RSI, Boulder, CO.
(19) Müller-Buschbaum, P.; Gutmann, J. S.; Wolkenhauer, M.; Kraus, J.; Stamm, M.; Smilgies, D.; Petry, W. *Macromolecules* **2001**, *34*, 1369−1375.
(20) MSDS: cyclohexane-d_{12}; OHS62652.
(21) MSDS: methyl isobutyl ketone; OHS14550.
(22) Grulke, E. A. Solutiblity Parameter Values. In *Polymer Handbook*, 3rd ed.; Brandrup, J., Immergut, E. H., Grulke, E. A., Eds.; Wiley: New York, 1989; Vol, II, p 675.

MA0115038